Laser-Pulse-Induced Second-Harmonic and Hard X-Ray Emission: Role of Plasma-Wave Breaking

A. S. Sandhu* and G. R. Kumar
Tata Institute of Fundamental Research, 1 Homi Bhabha Road, Mumbai 400 005, India

S. Sengupta, A. Das, and P. K. Kaw
Institute for Plasma Research, Bhat, Gandhinagar 382 428, India
(Received 29 August 2004; published 8 July 2005)

We report time resolved measurements of second-harmonic and hard x rays emitted during the interaction of an intense laser pulse (10^{16} W cm^{-2}, 100 fs) with a preplasma generated on a solid target. We observe that for a particular length scale the second harmonic goes through a minimum, while hard x-ray emission on the contrary maximizes. Theoretical or numerical modeling of this anticorrelation in terms of wave breaking of strongly driven electron plasma waves clearly brings out hitherto unexplored links between the physical mechanisms of second-harmonic generation and hard x-ray emission.

DOI: 10.1103/PhysRevLett.95.025005 PACS numbers: 52.25.Os, 52.35.Mw, 52.38.Kd, 52.38.Ph

The physics of interaction of an ultrashort high intensity laser pulse with a solid target is rich in nonlinear phenomena [1], like generation of harmonics [2], generation of fast particles and hard x rays [3–5], and the concomitant generation of multimegaguass magnetic fields [6]. Currently there is immense interest, both from a fundamental point of view and practical applications, in understanding the physics behind these phenomena. Insight into the mechanism of generation of hot electrons, harmonics, and hard x rays have important implications for the fast ignition concept of laser fusion [7], and other applications [8].

Fundamentally, the physical mechanism responsible for second-harmonic emission and hot electron generation (and hence hard x rays) is intimately related to the excitation and breaking of electron plasma waves excited at the critical layer through resonance absorption of the incident laser pulse. In this Letter we report our study, which for the first time experimentally illustrates this relationship. We present simultaneous time resolved measurements of laser light absorption, second-harmonic generation efficiency and hard x-ray yield as a function of plasma scale length. We demonstrate that this technique of looking for correlations between a nonlinear coherent process (harmonic generation) and an incoherent one (hard x-ray emission), as a function of various parameters like scale length, intensity, and polarization, provides clinching evidence of wave breaking and its effects on plasma processes. A detailed quantitative study reported here backed by self-consistent theoretical and numerical modeling clearly elucidates the effect of wave breaking on the emission of harmonics and x rays. These results also provide new pointers for control of harmonic and hot electron yields.

When a p-polarized light is incident on an inhomogeneous plasma slab, electron plasma waves are excited at the critical layer via a well-known resonance absorption mechanism [9]. The oscillatory energy contained in these electrostatic waves, gets damped through various collisional (like electron-ion collisions) and collisionless (like Landau damping) mechanisms and is converted into kinetic energy of hot electrons. These hot electrons then produce hard x rays through bremsstrahlung. Besides aiding the generation of hard x rays, the density oscillation of the excited plasma wave ($\delta n \sim \vec{\nabla} n^{(0)} e\vec{E}/m\omega^2\epsilon$) also nonlinearly couples with the oscillatory velocity of the plasma electrons ($\vec{v}_1 \sim e\vec{E}/m\omega^2$) resulting in a nonlinear current density $\vec{j}^{(2)} \sim -e\delta n\vec{v}_1$ which eventually radiates second harmonic of the incident light. Here $\vec{E}$ is the local electric field oscillating at frequency ω and ϵ is the local dielectric constant. It appears that, larger the amplitude of the excited plasma wave, larger should be the emission of hard x rays and second-harmonic radiation. The amplitude of the excited electrostatic wave (through its dependence on the fractional absorption f_a of the light wave) depends on the density scale length L/λ at the critical layer [9]; albeit the dependence may not be same as the dependence of f_a on L/λ. But it is expected that with increase in L/λ (for a fixed θ), the amplitude should increase, go though a maximum, and then decrease. This behavior of the plasma-wave amplitude with L/λ should also be reflected in the variation of x-ray generation and second-harmonic emission with L/λ.

The above physical picture is appropriate when oscillation energy is slowly drained out of the wave through linear mechanisms like Landau damping or electron-ion collisions. The situation drastically changes, when the damping process becomes nonlinear. It is well known that the amplitude of an electrostatic wave is limited by the wave breaking condition $k_p eE_z/m\omega^2 \sim 1$, where k_p and E_z are, respectively, the wave number and amplitude of the electrostatic wave at the critical layer [9,10]. Therefore for sufficiently high laser intensity, the excited plasma wave will most likely satisfy the wave breaking condition at the

point of maximum resonance absorption, leading to nonlinear damping of the wave. Physically, at wave breaking amplitudes the bulk of the background electrons are instantaneously ($\sim$ within a fraction of a plasma period) brought into resonance with the wave and are accelerated to velocities comparable to the phase velocity of the wave. The wave thus gets nonlinearly damped, its energy being efficiently converted into very energetic electrons which results in sharp enhancement in the hard x-ray emission. Interestingly, this nonlinear damping of the plasma wave through a wave breaking mechanism has an opposite effect on the second-harmonic emission. Physically, second-harmonic emission depends on the survival of the electrostatic wave. Since at the wave breaking point, the wave gets rapidly damped, the nonlinear current source $\vec{j}^{(2)}$ gets disrupted, resulting in a dip in the second-harmonic emission. This anticorrelation between hard x-ray emission and second-harmonic generation should therefore act as a sensitive indicator of the occurrence of wave breaking process. Previous studies, notably by Gizzi *et al.* [11] involving measurement of hard x-ray emission and second-harmonic efficiency as a function of polarization of the incident laser, have shown a dip in the second-harmonic efficiency when the incident light is nearly p polarized. These results were explained using similar arguments as above, albeit only qualitatively. Theoretically, wave breaking phenomenon has been much discussed since the seminal paper by Dawson [10]. Experimentally, however, besides the work by Gizzi *et al.* and a few others [5] who have invoked wave breaking briefly and qualitatively, there does not exist any experimental study that has dealt with this important phenomenon directly. Thus, to our knowledge, ours is the first experimental study that quantitatively establishes wave breaking and its link with hot electron, hard x-ray and second-harmonic generation.

Our experimental setup consists of a main pulse (10^{16} W cm^{-2}, 100 fs, 800 nm) incident at an angle of 45° with respect to the target normal. The prepulse which forms a plasma on the target surface is 50 times weaker than the main pulse, and is incident normally on the target. The target used is BK7 glass of 2 in $\times$ 2 in $\times$ 5 mm in size. The scale length of the plasma is varied in a controlled manner by changing the time delay between the main pulse and the prepulse via a precise translation stage. Using photodiodes (Hamamatsu), we monitor the input laser fluctuation, reflection coefficient of the prepulse, and reflection coefficient of the main pulse. The second harmonic generated by the main pulse is monitored with a photomultiplier tube (Hamamatsu) and with a spectrometer coupled to a CCD. A NaI (Tl) detector appropriately gated with respect to the laser pulse and placed at 22.5° with respect to the target normal is used to measure the hard x-ray emission in the energy range from 30 to 300 keV.

We now present our experimental results on hard x-ray and second-harmonic measurements as a function of the prepulse to main pulse time delay at fixed polarization (p polarization) of the main pulse in Figs. 1(a) and 1(b). We have plotted integrated hard x-ray yield over 30–300 keV energy range [Fig. 1(a)] and second-harmonic efficiency $\eta \propto I(2\omega)/I^2(\omega)$ [Fig. 1(b)], as a function of the time delay (bottom axis). In both the plots the data are normalized with respect to yields obtained with main pulse acting alone. The hard x-ray yield shows an initial rise, a maximum around $\sim$24 ps, and finally a slow decay for large values of time delay. The second-harmonic efficiency η shows similar behavior for small and large time delay. The most interesting feature, however, is the observed dip in second-harmonic efficiency around the same point where hard x-ray emission maximizes. Around $\sim$24 ps, second-harmonic efficiency dips to half its maximum value, whereas the hard x-ray yield is enhanced by 2 orders of magnitude as compared to its baseline value, indicating a large amount of hot electron generation. To establish that there is indeed copious generation of hot electron current around $\sim$24 ps, we have performed spectrally resolved hard x-ray measurements. The energy resolved spectra show a good fit to double exponential decay of the form $N(E) = A_1 \exp(-E/T_1^{\text{hot}}) + A_2 \exp(-E/T_2^{\text{hot}})$, where T_1^{hot} and T_2^{hot} are two hot electron components and A_1 and A_2 are their relative weights. The results are summarized in

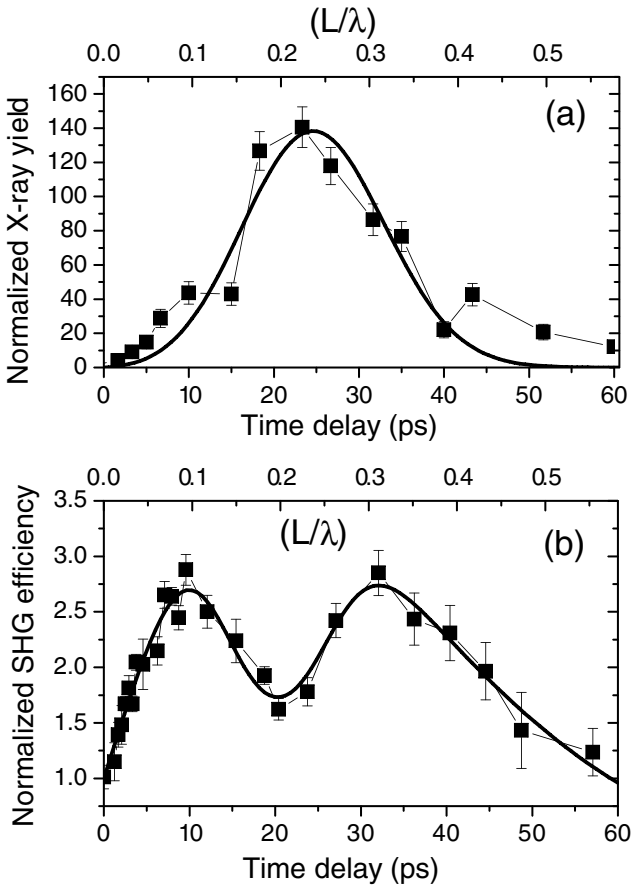

FIG. 1. (a) Integrated yield of x rays from 30 to 300 keV (b) Second-harmonic efficiency, each normalized with respect to yield in the absence of a prepulse, as a function of time delay.

Table I. The first row corresponds to the case when main pulse is acting alone and the second row corresponds to the case when the prepulse to main pulse delay is ~24 ps. Comparison of the hot electron temperatures shows a very prominent high temperature component in the second case, indicating a burst in hot electron current generation at the scale length corresponding to 24 ps delay.

The variation of hard x-ray yield [Fig. 1(a)] and second-harmonic efficiency η [Fig. 1(b)] with time delay, and the hot electron temperatures at ~24 ps is strongly indicative of the occurrence of physical mechanisms described earlier. To further substantiate our physical picture, we have also simultaneously measured the reflectivity of the main pulse as a function of time delay [see Fig. 2(a)]. As expected, with the increase in scale length, resonance absorption initially increases, with broad maximum at time delays where second-harmonic emission dips and hard x-ray yield peaks, and then decreases for larger values of time delay. Hence we conclude that around 24 ps delay large amplitude electrostatic waves are being excited and undergo nonlinear damping via wave breaking mechanism thus producing large amount of hot electrons, resulting in a peak in x-ray emission and a dip in second-harmonic generation. We also note here that the second-harmonic emission was observed to be specular in our experiments, another indication of the fact that second-harmonic radiation is generated by electron plasma waves produced by a linear conversion mechanism like resonance absorption.

We now present a theoretical analysis and model our results in terms of resonance absorption and wave breaking. We model the x-ray yield as a quantity Y which is taken to be proportional to the intensity of the absorbed light $I_{\mathrm{abs}} = \int_0^\infty \nu_{\mathrm{eff}} E_z^2/8\pi dz$, where ν_{eff} is the effective rate at which energy is drained out of the plasma wave through linear/nonlinear processes and E_z is the electric field associated with the plasma wave. It is well known that for $\nu_{\mathrm{eff}}/\omega \rightarrow 0$ (linear processes) intensity of the absorbed light is independent of the process of absorption. In general, however, for nonlinear processes intensity of the absorbed light is dependent on the process of absorption. This is because the amplitude of the excited plasma wave, as it approaches the resonance region, instead of increasing as $E_z \sim 1/\epsilon$, gets clamped to the value dictated by the wave breaking condition $k_p e E_{\mathrm{WB}}/(m\omega_p^2) \sim 1$, where $k_p \sim (\lambda_D^2 L)^{-1/3}$ is the wave number of the plasma wave. Therefore, the absorption integral can be written as $I_{\mathrm{abs}} \approx \int_0^l \nu_{\mathrm{eff}} \frac{E_z^2}{8\pi} dz + \int_l^\infty \nu_{\mathrm{eff}} \frac{E_{WB}^2}{8\pi} dz$ where $E_{\mathrm{WB}} \sim m\omega_p^2(\lambda_D^2 L)^{1/3}/e$ and "l" is the point of initiation of wave breaking. We believe that it is the second integral which contributes maximally to the x-ray yield which may be approximated as $\int_l^\infty \nu_{\mathrm{eff}} \frac{E_{\mathrm{WB}}^2}{8\pi} dz \approx \nu_{\mathrm{eff}} \frac{m^2\omega_p^4}{8\pi e^2}(\lambda_D^2 L)^{2/3} \times (\lambda_D^2 L)^{1/3} \sim \nu_{\mathrm{eff}} L$, where the range of integration is taken as wavelength of the plasma wave near the resonant region. These arguments give a phenomenological expression of x-ray yield as

$$Y = A(L/\lambda)_{\mathrm{cr.}} f(L/\lambda)_{\mathrm{cr.}} \tag{1}$$

where A is some proportionality constant and $\nu_{\mathrm{eff}} = f(L/\lambda)_{\mathrm{cr.}}$ is an unknown function of the argument, which is to be determined from experiments. For second-harmonic efficiency η, we use the model developed by Erokhin *et al.* [12], which gives the scaling of second-harmonic efficiency η with $(L/\lambda)_{\mathrm{cr.}}$ and $(\nu_{\mathrm{eff}}/\omega)_{\mathrm{cr.}}$ as

$$\eta \propto \rho^2 \exp[-(b + d(\nu_{\mathrm{eff}}/\omega)_{\mathrm{cr.}})\rho] \tag{2}$$

where $\rho = 2\pi(L/\lambda)_{\mathrm{cr.}}$ and "b" and "d" are two constants of order unity. Although Erokhin's model [12] is strictly valid under the assumptions of long gradient scale length ($\frac{2\pi L}{\lambda} \gg 1$) and weak nonlinearity, the form of Eq. (2) does not change even if these assumptions are violated. This is because the form of energy flow in the second harmonic which is given by $\langle \vec{S}_2 \rangle = \frac{c}{8\pi}\langle \vec{E}_2 \times \vec{H}_2^* \rangle$ depends on exponentially dropping fields; and the fact that the second-

TABLE I. Comparison of two hot electron temperatures obtained without prepulse and with prepulse at 24 ps. Also given is relative weightage of second temperature component.

Delay (ps)	T_1^{hot} (keV)	T_2^{hot} (keV)	A_2/A_1
0	3 ± 0.4	20 ± 8	5×10^{-5}
24	5 ± 0.5	37 ± 7	1×10^{-3}

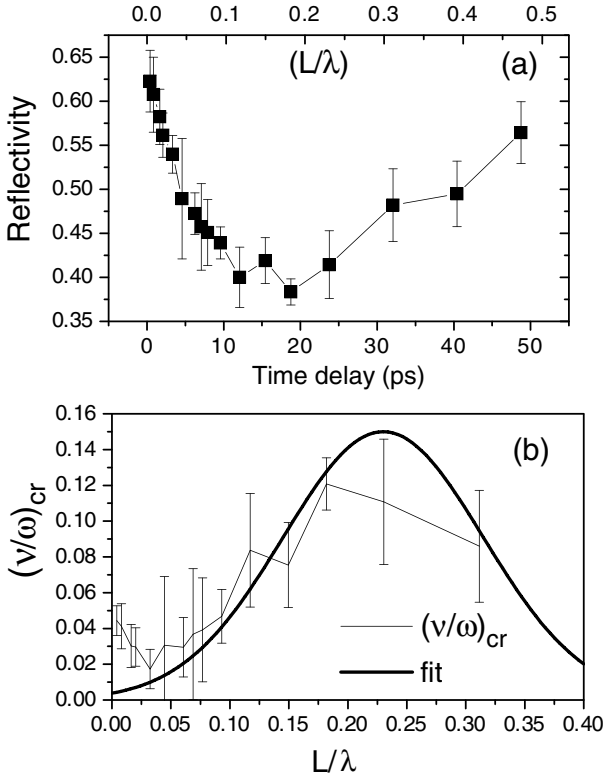

FIG. 2. (a) Reflectivity of the pump pulse with delay (scale length) of the preplasma. (b) Variation of effective damping term $(\nu_{\mathrm{eff}}/\omega)_{\mathrm{cr.}}$ with L/λ.

harmonic fields ($\vec{E}_2, \vec{H}_2$) are exponentially decaying do not depend on the assumptions of long gradient scale length and small nonlinearity. Thus in the absence of a detailed theory, we have adopted Erokhin's model [12] in a phenomenological fashion, using only the scale dependence and evaluating the parameters from experimental fit. We now evaluate these parameters ($(L/\lambda)_{\text{cr.}}$ & $(\nu_{\text{eff}}/\omega)_{\text{cr.}}$) from the reflectivity curve of the main pulse [Fig. 2(a)]. Using the condition for maximum resonance absorption as $(2\pi(L/\lambda)_{\text{cr.}})^{1/3}\sin\theta \sim 0.8$, we make an estimate of $(L/\lambda)_{\text{cr.}} \approx 0.23$. This value of $(L/\lambda)_{\text{cr.}}$ corresponds to the time delay when resonance absorption maximizes ($\sim$24 ps). This in turn, gives an estimate of the expansion velocity $v_{\text{exp}} \sim 8 \times 10^5$ cm/sec at prepulse intensity $\sim 2 \times 10^{14}$ W/cm^2, which compares very well with the direct estimation of velocity through Doppler shift measurements [13]. Using this expansion velocity, the time delay axis is calibrated with corresponding scale length values at the critical layer $(L/\lambda)_{\text{cr.}}$ (see top axis of Figs. 2(a), 1(a), and 1(b)]. This yields a very good estimate of scale lengths as shown by actual measurements in glass samples by Bastiani *et al.* [5].

Reflectivity as a function of scale length $(L/\lambda)_{\text{cr.}}$ is now utilized to evaluate the effective damping coefficient $(\nu_{\text{eff}}/\omega)_{\text{cr.}}$, for each value of reflectivity by numerically solving the wave equation for complex magnetic field $\tilde{B}$ of a p-polarized light propagating through an inhomogeneous plasma slab *viz.*, $\frac{d^2\tilde{B}}{dz^2} + k^2(\epsilon(z) - \sin^2\theta) - \frac{1}{\epsilon}\frac{d\epsilon}{dz}\frac{d\tilde{B}}{dz} = 0$ [14,15]. Here "z" is the direction of the density inhomogeneity and $\epsilon = 1 - \xi + i\xi\nu/\omega$ with $\xi = (\omega_p^2/\omega^2(z)) \times (1 + \nu^2/\omega^2(z))^{-1}$ is the complex dielectric constant. Choosing a linear density profile and taking $\nu(z)/\omega$ as proportional to density, we numerically evaluate the reflectivity of the main pulse for each value of $(L/\lambda)_{\text{cr.}}$ treating $(\nu_{\text{eff}}/\omega)_{\text{cr.}}$ as a parameter [15]. Matching the calculated value of reflectivity with the observed value gives $(\nu_{\text{eff}}/\omega)_{\text{cr.}}$ as a function of $(L/\lambda)_{\text{cr.}}$ as shown in Fig. 2(b). The error bars in this figure correspond to the error bars in the reflectivity curve. The high value of $(\nu_{\text{eff}}/\omega)_{\text{cr.}} \sim 0.15$ (this is an order of magnitude higher than (ν_{ei}/ω) for $T_e \approx$ 100 eV, which is typically the bulk temperature at our intensities) at the peak, corresponding to the maxima of resonance absorption satisfies the wave breaking condition $[eH(0)/mc\omega]/[(\rho/\alpha_0)(\nu_{\text{eff}}/\omega)^2] \sim 1$ where $\alpha_0 = \sin\theta$ [9,12] and hence gives a clear indication of damping of the excited electrostatic waves at the critical layer by wave breaking. These values of $(\nu_{\text{eff}}/\omega)_{\text{cr.}}$ are now used to fit the x-ray yield and second-harmonic efficiency η according to the models described by Eqs. (1) and (2). To do this, we first represent the gross behavior of $(\nu_{\text{eff}}/\omega)_{\text{cr.}}$ as a function of $(L/\lambda)_{\text{cr.}}$ obtained numerically with a smooth function of the form $(\nu_{\text{eff}}/\omega)_{\text{cr.}} = a\exp[-((L/\lambda)_{\text{cr.}} - c)^2/w^2]$ with $a \sim 0.15$, $c \sim 0.2$, and $w \sim 0.1$ (solid line in Fig. 2(b)]. We use this Gaussian form in Eqs. (1) and (2) to fit the hard x-ray yield "Y" and the second-harmonic efficiency η. The excellent fits obtained for both Y and η [see the solid lines in Figs. 1(a) and 1(b)], clearly vindicates the physical model described in this Letter.

In conclusion, we have done simultaneous time resolved study of hard x-ray yield and second-harmonic emission from laser produced plasmas as a function of plasma scale length. The observed anticorrelation of x-ray generation with second-harmonic emission as a function of scale length, exhibits a clean signature of wave breaking. In fact, our experimental work represents first one of its kind where onset of wave breaking has been dynamically timed by varying the prepulse to main pulse time delay. Theoretical or numerical modeling of our experimental results is in good agreement with the theory of resonance absorption and wave breaking, and thus has clearly brought out the role played by wave breaking of large amplitude plasma waves, in hot electron generation, hard x-ray emission and second-harmonic generation. Our data further highlights the effect of wave breaking in limiting the second-harmonic generation and shows that increasing the laser intensity for enhancing second harmonic would fail to be very productive in absence of proper optimization and this optimization is very different, in fact quite opposite to what is observed for x-ray yields.

*Present address: JILA, University of Colorado, Boulder, CO 80309, USA
arvinder@jilau1.colorado.edu

[1] P. Gibbon and E. Forster, Plasma Phys. Controlled Fusion **38**, 769 (1996).
[2] D. von der Linde *et al.*, IEEE J. Quantum Electron. **28**, 2388 (1992); A. Tarasevitch *et al.*, Phys. Rev. A **62**, 023816 (2000); M. Zepf *et al.*, Phys. Rev. E **58**, R5253 (1998).
[3] M. Hegelich *et al.*, Phys. Rev. Lett. **89**, 085002 (2002); H. Habara *et al.*, Phys. Rev. E **69**, 036407 (2004); V. Kumarappan *et al.*, Phys. Rev. Lett. **87**, 085005 (2001).
[4] J. D. Kmetec *et al.*, Phys. Rev. Lett. **68**, 1527 (1992); Y. Sentoku *et al.*, Phys. Plasmas **6**, 2855 (1999); A. A. Andreev *et al.*, Phys. Rev. E **65**, 026403 (2002).
[5] S. Bastiani *et al.*, Phys. Rev. E **56**, 7179 (1997); Th. Schelgel *et al.*, Phys. Rev. E **60**, 2209 (1999).
[6] A. S. Sandhu *et al.*, Phys. Rev. Lett. **89**, 225002 (2002); Z. Najmudin *et al.*, Phys. Rev. Lett. **87**, 215004 (2001).
[7] R. Kodama *et al.*, Nature (London) **412**, 798 (2001).
[8] C. Rischel *et al.*, Nature (London) **390**, 490 (1997); K.-S Tinten *et al.*, Nature (London) **422**, 287 (2003); P. Gibbon, Phys. Rev. Lett. **76**, 50 (1996).
[9] W. L. Kruer, *The Physics of Laser-Plasma Interactions* (Addison-Wesley, New York, 1988).
[10] J. M. Dawson, Phys. Rev. **113**, 383 (1959).
[11] L. A. Gizzi *et al.*, Phys. Rev. Lett. **76**, 2278 (1996).
[12] N. S. Erokhin *et al.*, Sov. Phys. JETP **29**, 101 (1969).
[13] B. -T. V. Vu *et al.*, Phys. Rev. Lett. **72**, 3823 (1994).
[14] H. M. Milchberg and R. R. Freeman, J. Opt. Soc. Am. B **6**, 1351 (1989).
[15] H. M. Milchberg *et al.*, Phys. Rev. Lett. **61**, 2364 (1988).